Supporting Information

Modulating the morphology of gold graphitic nanocapsules for plasmon resonance-enhanced multimodal imaging

Xiao-Fang Lai[†], Yu-Xiu Zou[†], Shan-Shan Wang[†], Meng-Jie Zheng[‖], Xiao-Xiao Hu[†], Hao Liang[†], Yi-Ting Xu[†], Xue-Wei Wang[†], Ding Ding[†], Long Chen[§], Zhuo Chen[†,*], Weihong Tan[†,*]

[†]Molecular Sciences and Biomedicine Laboratory, State Key Laboratory for Chemo/Biosensing and Chemometrics, College of Chemistry and Chemical Engineering, College of Biology and Collaborative Innovation Center for Molecular Engineering and Theranostics, Hunan University, Changsha 410082, China.

[‖] School of Physics and Microelectronic Science, Hunan University, Changsha 410082, China.

[§]Faculty of Science and Technology, University of Macau, E11, Avenida da Universidade, Taipa, Macau, China.

*Email: zhuochen@hnu.edu.cn; tan@chem.ufl.edu.

Experimental details:

Dynamic light scattering characterization of Au@G and AuNR@G

The hydrodynamic diameters of the nanoparticles under investigation were measured using a Zetasizer Nano ZS90 DLS system equipped with a red (633 nm) laser and an Avalanche photodiode detector (APD) (quantum efficiency > 50% at 633 nm) (Malvern Instruments Ltd., Worcestershire, England). DLS measurements were performed at room temperature at a fixed scattering angle of 90°. All size distributions reported here were based on number counting. The average particle size was obtained using a non-negative least squares (NNLS) analysis method. For each sample, two DLS measurements were conducted with a fixed 11 runs, and each run lasted 10 s.

ζ-Potential measurement of Au@G and AuNR@G

Zeta-Potential measurements were performed in water. The measurements were carried out at room temperature on the ZetaSizer Nano ZS90 equipped with MPT-2 Autotitrator and 4 mW He-Ne Laser (λ_0= 633 nm) using the Laser Doppler Electrophoresis technique. Zeta-potential was calculated by Dispersion Technology software provided by Malvern according to Smoluchowski approximation in an automatic mode. Figure S3 shows the Zeta-potential curves of the Au@G and AuNR@G water solution.

Stability tests of the AuNR@Gs

To further investigate the stability of AuNR@Gs in biological medium, DMEM medium supplemented with 10% premium fetal bovine serum (FBS) and 1% penicillin-streptomycin was used. The photos of AuNR@Gs in H_2O, DPBS and DMEM in 3 hours were shown in Figure S3. UV-Vis characterization was utilized to monitor morphological changes. AuNR@G has better Raman signals compared with the organic Raman dye. Figure S5 showed that the Raman signals of R6G fade away when added reducing agent 0.1 M $NaBH_4$, but the Raman signals of AuNR@Gs did not change.

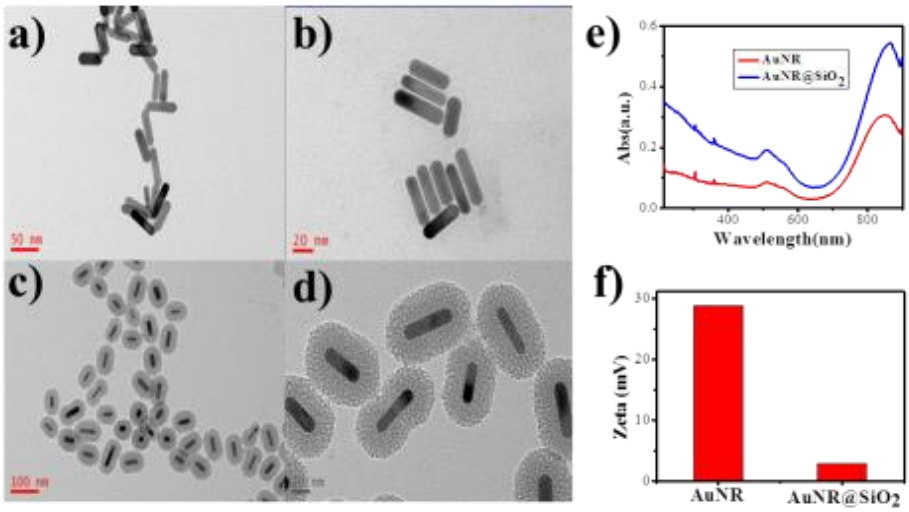

Figure S1. Characterization of synthetic nanocomposites. (a) and (b) TEM image of AuNRs; (c) and (d) TEM image of AuNR@SiO_2; (e) UV-Vis spectra of AuNR (red line) and AuNR@SiO_2 (blue line); (f) ζ-potential value of AuNR and AuNR@SiO_2.

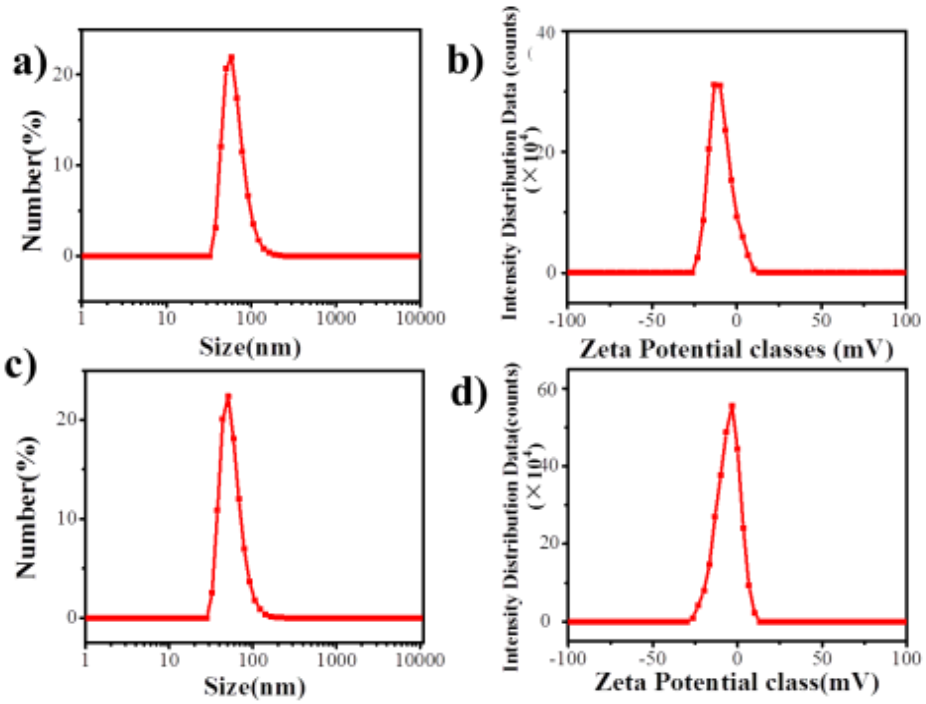

Figure S2. DLS characterization of the size distribution of AuNR@G (a) and Au@G (c); ζ-potential curves of AuNR@G (b) and Au@G (d) measured at room temperature on the ZetaSizer Nano ZS90.

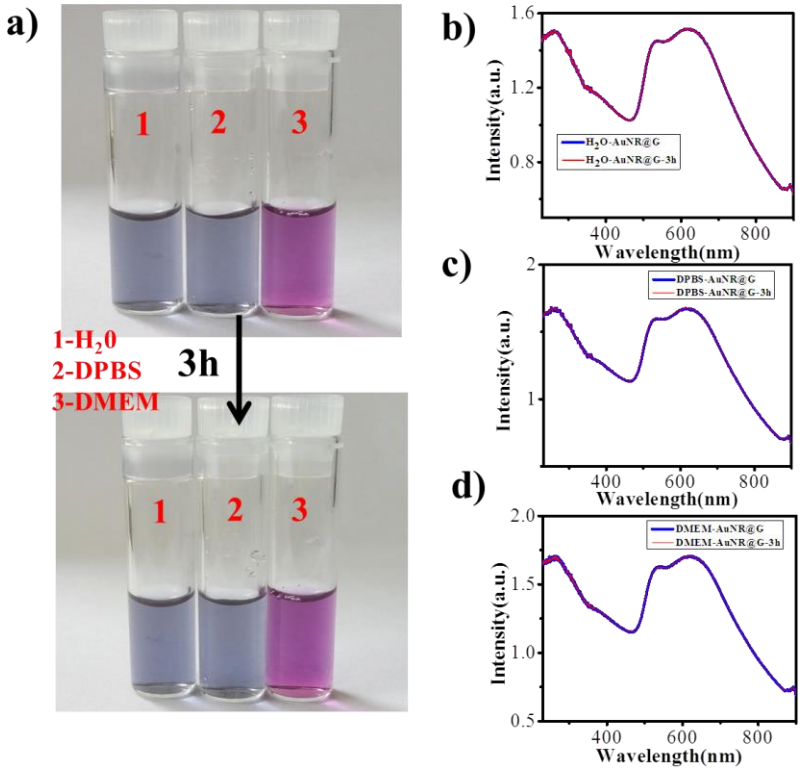

Figure S3.The stability of AuNR@G nanocapsules. (a) Digital photos of AuNR@G in H_2O, DPBS and DMEM solution; (b), (c), and (d), UV-Vis spectra of AuNR@G in H_2O, DPBS and DMEM before and after 3 h incubation, respectively.

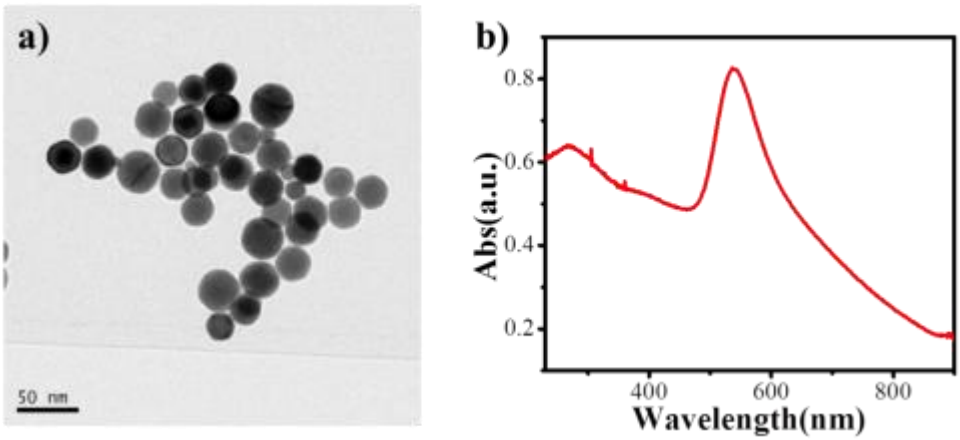

Figure S4. (a) Transmission electron microscopy characterization of Au@G; (b) UV-Vis spectrum of aqueous Au@G.

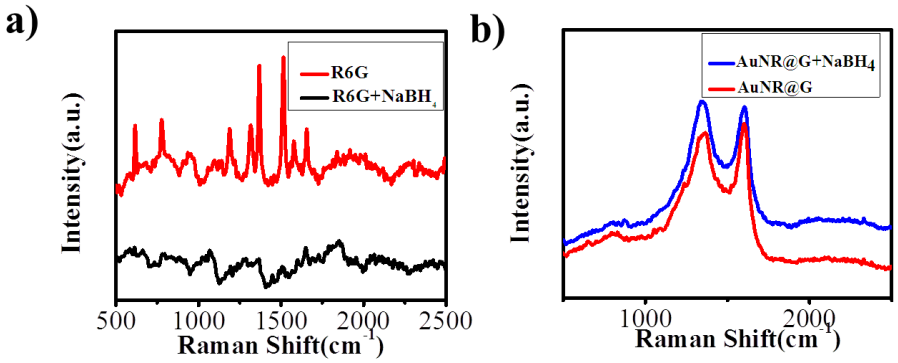

Figure S5. The stability of Raman signals of AuNR@G and R6G. (a) Raman spectra of R6G, with and without 0.1 M $NaBH_4$; (b) Raman spectra of AuNR@G, with and without 0.1 M $NaBH_4$. Excitation at 633 nm.

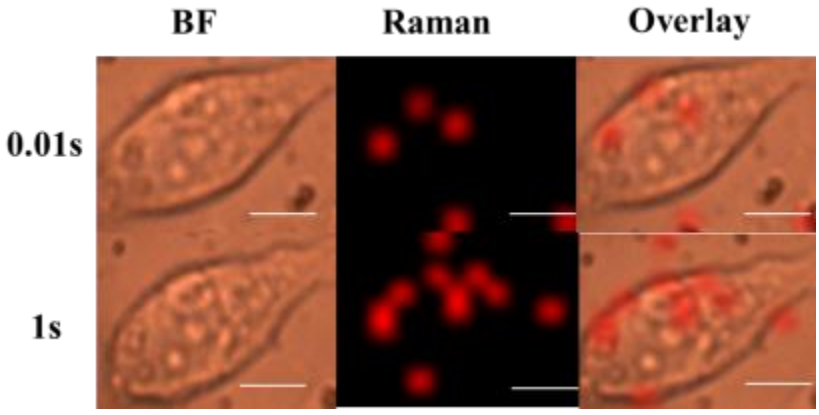

Figure S6. Rapid Raman mapping image of MCF-7 cells with and without Au@G staining using 0.01 s and 1 s integration/pixel, respectively. BF: bright field; scale bar: 10 μm.

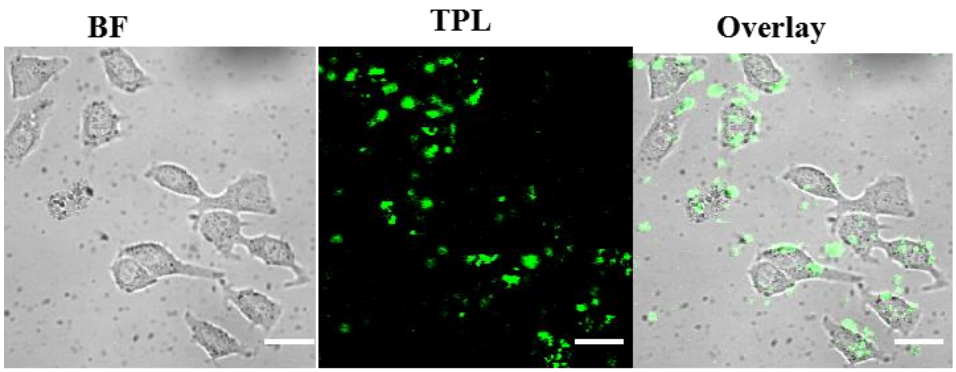

Figure S7. TPL confocal images of MCF-7 cells stained with Au@G. BF: bright field; scale bar: 50 μm.